Available online at www.sciencedirect.com
SCIENCE DIRECT®
Journal of Sound and Vibration 271 (2004) 131–146
JOURNAL OF SOUND AND VIBRATION
www.elsevier.com/locate/jsvi

Free vibrations of rectangular cantilever plates. Part 1: out-of-plane motion

Jongwon Seok*, H.F. Tiersten, H.A. Scarton

Department of Mechanical, Aerospace and Nuclear Engineering, Rensselaer Polytechnic Institute, 110 8th Street, Troy, NY 12180-3590, USA

Received 9 May 2002; accepted 26 February 2003

Abstract

An analysis of the free transverse vibrations of a cantilevered plate is performed by means of a variational approximation procedure. Since the variational equation with all natural conditions is available for the three-dimensional elastic equations but not for the plate equation, the required variational equation for the plate is obtained by means of a low order expansion in the three-dimensional equation. The uncoupled flexural portion of the resulting system is used in the problem treated in this work. The problem is treated by first obtaining the exact solution for flexural waves in the thin plate by satisfying the flexural equation for the plate with two opposite edges free. The solution results in a set of dispersion curves. A number of the resulting waves are used in what remains of the variational equation, in which all conditions occur as natural conditions. Roots of the resulting transcendental equation are calculated, which yield the eigensolutions and associated eigenfrequencies. The results compare very well with those from finite element method treatment, which shows that this procedure is very accurate. It also provides an understanding in terms of the waves that make up the vibration, which is not provided by any of the other methods.

1. Introduction

It is well known that the problem of the transverse vibrations of a cantilever beam can be solved exactly. However, if the width of the configuration is relatively large, it can no longer be treated as a beam, but must be treated as a plate. Although the transverse vibrations of a plate can be treated exactly if two opposite edges are simply supported, it cannot be treated exactly for many other

*Corresponding author. Tel.: +1-518-276-8003; fax: +1-518-276-8761.
E-mail address: seokj@alum.rpi.edu (J. Seok).

0022-460X/03/$ - see front matter © 2003 Elsevier Ltd. All rights reserved.
doi:10.1016/S0022-460X(03)00365-1

cases. Consequently, the problem of a rectangular cantilever plate free on the other three edges must be treated by some form of approximation procedure. For this reason, the free vibration problems for a thin elastic cantilever plate have been studied over the past few decades using some form of approximation procedure, such as the Ritz or Rayleigh–Ritz method with beam functions [1,2], with characteristic orthogonal polynomials [3], or by using finite element method (FEM) [4]. Gorman [5] used Fourier series along with superposition to treat this problem for the isotropic case, and later, extended his work to the orthotropic case [6].

In this work, a variational approximation procedure is used, in which the differential equation and the edge conditions on either side of the width are satisfied exactly and the edge conditions at the free and fixed edges are satisfied variationally. The motivation for using this procedure is to satisfy as much of the problem exactly as possible while leaving the remainder to be satisfied variationally, using as small a number of the exact solution functions as are needed to obtain the accuracy required. The procedure is semi-analytical and provides some understanding through the values of the amplitudes of the exact solution functions used, whereas FEM and the Rayleigh–Ritz method yield only the final numbers that result. The variational equation for the classical theories of plates, in which all conditions, i.e., those of both natural and constraint types, arise as natural conditions, is not readily available. However, since such three-dimensional equations are available, the two-dimensional variational equation for the flexural vibrations of thin plates is derived from the existing three-dimensional formulation. Naturally, the conditions of both natural and constraint types in the resulting two-dimensional variational equation arise as natural conditions. This is done by making a low order expansion of the displacement in the thickness co-ordinate and integrating through the thickness in the manner of Mindlin [7]. The equations are obtained for orthotropic symmetry, in which three-dimensional shear and extension are not coupled. Following Mindlin, the vertical plate shearing strains are taken to vanish and the vertical plate shear constitutive equations are ignored in order to reduce the description to the classical equation of flexure consisting of one differential equation in one variable, which is the deflection.

The exact solution of the differential equation and free edge conditions on either side of the width yields dispersion curves. The dispersion curves for two-dimensional flexure of thin plates presented in this work are exact and to our knowledge have not appeared in the literature before. Up to eight of these solutions are taken, which are represented by the dispersion curves in what remains of the variational equation with all natural conditions, including Kirchhoff's well-known corner conditions, to obtain a system of linear homogeneous algebraic equations, which enables the calculations to be performed. Among other things, the calculations clearly show the dependence of the natural frequencies on the width of the plate for a given length. The results compare favorably with those in the isotropic literature [1] and with finite element analysis [8].

2. Variational equation for the motion of a thin orthotropic plate

As mentioned in the Introduction, the two-dimensional equations for the thin plate will be derived from the available three-dimensional variational equation. Thus, it is informative to begin with the modified form of Hamilton's principle, in which Lagrange multipliers were introduced to eliminate constraint conditions and have them arise as natural conditions [9,10], which may be

written in the form

$$\int_{t_0}^{t} \mathrm{d}t \left[\int_V (\tau_{ij,i} + \bar{f}_j - \rho \ddot{u}_j) \delta u_j \, \mathrm{d}V + \int_{S_N} (\bar{t}_j - n_i \tau_{ij}) \delta u_j \, \mathrm{d}S + \int_{S_C} n_i (u_j - \bar{u}_j) \delta \tau_{ij} \, \mathrm{d}S \right] = 0, \tag{1}$$

where indicial tensor notation has been employed along with the conventions that a comma followed by an index denotes partial differentiation with respect to the space co-ordinate x_i ($i = 1$, 2, 3) indicated by the index, a dot over a variable denotes partial differentiation with respect to time and repeated tensor indices are to be summed. In this equation, the symbols V and ρ stand for the volume occupied by the body and the mass density, respectively, S_N, S_C denote, respectively, the portion of the surface on which natural- and constraint-type conditions are prescribed, τ_{ij}, u_j and n_i denote the components of the stress tensor, mechanical displacement and unit outward normal vectors, respectively, $\bar{t}_j, \bar{f}_j$ and $\bar{u}_j$ represent the components of the prescribed traction, body force and mechanical displacement vectors, respectively. Note that the first term in Eq. (1) corresponds to the stress equations of motion, the second term to the boundary conditions on the portion of the surface on which the traction is prescribed and the third term to the boundary conditions on the portion of the surface on which the mechanical displacement is prescribed. Furthermore, it is assumed in this work that the system obeys the linear constitutive equations

$$\tau_{ij} = c_{ijkl} \varepsilon_{kl}, \tag{2}$$

and, of course, the infinitesimal strain–displacement relations are given by

$$\varepsilon_{kl} = \tfrac{1}{2}(u_{k,l} + u_{l,k}), \tag{3}$$

where ε_{kl}, c_{ijkl} denote the components of strain and elastic constants, respectively. It should be noted that the material employed in this work is assumed to have orthotropic symmetry with respect to the co-ordinate axes so that extension is not coupled with shear in the three-dimensional equations.

Consider a fixed Cartesian co-ordinate system x_i with the faces of the plate of area S, at $x_3 = \pm h$. The axes x_1 and x_2 are co-ordinates lying in the mid-plane, intersecting the right prismatic boundary of the plate in a line path c and the origin of the co-ordinate is as shown in Fig. 1(a). Fig. 1(b) represents an element of the rectangular plate showing the relevant stress resultants required in the description of both flexure and extension of the plate.

Following Mindlin [7], the two-dimensional plate equation can be obtained by expanding the displacement in a sum of powers of the thickness co-ordinate of the plate thus

$$u_b = \sum_{n=0}^{1} x_3^n u_b^{(n)}(x_a, t), \quad u_3 = \sum_{n=0}^{2} x_3^n u_3^{(n)}(x_a, t), \tag{4}$$

where the convention has been employed that the indices a, $b = 1$ or 2 but not 3.

The substitution of the expansions in Eq. (4) into Eq. (3) yields the strains in terms of a sum of Mindlin's plate strains $\varepsilon_{ij}^{(n)}$ [7] in the form

$$\varepsilon_{ab} = \sum_{n=0}^{1} x_3^n \varepsilon_{ab}^{(n)}, \quad \varepsilon_{33} = \sum_{n=0}^{1} x_3^n \varepsilon_{33}^{(n)}, \quad \varepsilon_{3a} = \sum_{n=0}^{2} x_3^n \varepsilon_{3a}^{(n)}, \tag{5}$$

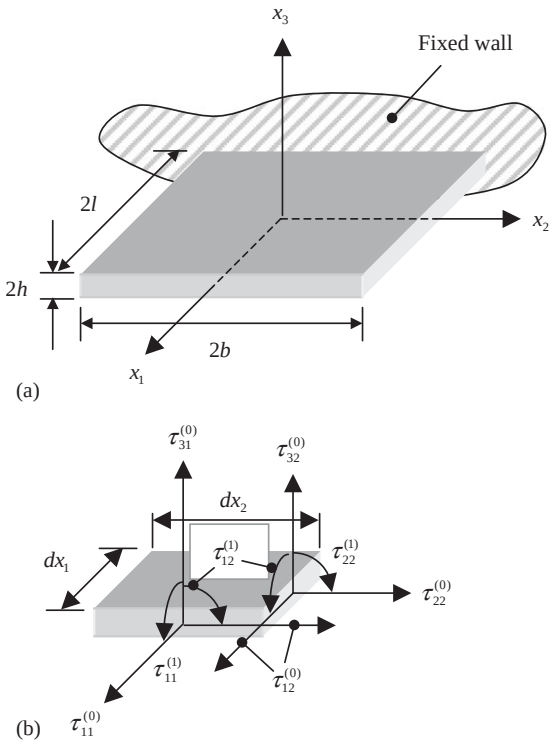

Fig. 1. A schematic of rectangular plate: (a) three-dimensional view of the rectangular cantilever plate and (b) an element of the rectangular plate.

where

$$\varepsilon_{ij}^{(n)} = \tfrac{1}{2}\Big\{u_{i,j}^{(n)} + u_{j,i}^{(n)} + (n+1)(\delta_{3i}u_j^{(n+1)} + \delta_{3j}u_i^{(n+1)})\Big\}, \tag{6}$$

which enables us to write

$$\varepsilon_{ab}^{(n)} = \tfrac{1}{2}(u_{a,b}^{(n)} + u_{b,a}^{(n)}), \quad \varepsilon_{33}^{(n)} = (n+1)u_3^{(n+1)}, \quad \varepsilon_{3a}^{(0)} = \varepsilon_{a3}^{(0)} = \tfrac{1}{2}(u_{3,a}^{(0)} + u_a^{(1)}), \tag{7}$$

if $u_3^{(1)}$ and $u_3^{(2)}$ are ignored, which will be done shortly by allowing for the free thickness expansion of the plate.

The substitution of Eq. (4) into Eq. (1), while performing of the integrations with respect to x_3 between the limits $x_3 = \pm h$, and the integration by parts of the terms differentiated with respect to x_3, yields the variational equation for the thin plate, which can be written in the form

$$\int_S \mathrm{d}S\left[\sum_{n=0}^{1}\left(\tau_{ab,a}^{(n)} - n\tau_{3b}^{(n-1)} + \bar{F}_b^{(n)} - \rho\sum_{m=0}^{1}\hat{\Theta}^{(m,n)}\ddot{u}_b^{(m)}\right)\delta u_b^{(n)} + \sum_{n=0}^{2}\left(\tau_{a3,a}^{(n)} - n\tau_{33}^{(n-1)} + \bar{F}_3^{(n)} - \rho\sum_{m=0}^{2}\hat{\Theta}^{(m,n)}\ddot{u}_3^{(m)}\right)\delta u_3^{(n)}\right]$$

$$+\int_{c_N} \mathrm{d}s\left[\sum_{n=0}^{1}(\bar{t}_b^{(n)} - n_a\tau_{ab}^{(n)})\delta u_b^{(n)} + \sum_{n=0}^{2}(\bar{t}_3^{(n)} - n_a\tau_{a3}^{(n)})\delta u_3^{(n)}\right]$$

$$+\int_{c_C} \mathrm{d}s\left[\sum_{n=0}^{1} n_a(u_b^{(n)} - \bar{u}_b^{(n)})\delta\tau_{ab}^{(n)} + \sum_{n=0}^{2} n_a(u_3^{(n)} - \bar{u}_3^{(n)})\delta\tau_{a3}^{(n)}\right] = 0, \tag{8}$$

where S is the area of the plate, c_N stands for the portion of the edges on which the traction is prescribed and c_C represents the portion of the edges on which the mechanical displacement is prescribed, and the time integration has been ignored since it is not needed in this work. In Eq. (8), the definitions

$$\tau_{ij}^{(n)} = \int_{-h}^{h} \tau_{ij} x_3^n \,\mathrm{d}x_3, \tag{9}$$

$$\bar{F}_j^{(n)} = \int_{-h}^{h} \bar{f}_j x_3^n \,\mathrm{d}x_3 + \left[\tau_{3j} x_3^n\right]_{x_3=-h}^{x_3=h}, \tag{10}$$

$$\bar{t}_j^{(n)} = \int_{-h}^{h} \bar{t}_j x_3^n \,\mathrm{d}x_3 \tag{11}$$

have been employed, where $\tau_{ij}^{(n)}$, $\bar{F}_j^{(n)}$ and $\bar{t}_j^{(n)}$are the nth order components of the stress resultants, body force resultants, prescribed traction resultants on c_N, respectively, and $\bar{u}_j^{(n)}$ are the nth order components of prescribed displacement on c_C, and

$$\hat{\Theta}^{(m,n)} = \int_{-h}^{h} x_3^{m+n} \,\mathrm{d}x_3 = \left[\frac{x_3^{m+n+1}}{m+n+1}\right]_{-h}^{h} \tag{12}$$

represents the shown integral, which vanishes for $m+n$ odd, and the notation

$$[f(x)]_{x=p}^{x=q} = f(q) - f(p)$$

has been employed.

For notational convenience, the usual compressed matrix notation will be employed hereafter according to the scheme given in Table 1. Then, the linear constitutive Eq. (2) can be expressed in the more compact form [11]

$$\tau_p = c_{pq}\varepsilon_q, \quad p,q = 1,2,\ldots,6, \tag{13}$$

where $c_{pq} \triangleq c_{ijkl}$ are the elastic stiffnesses, and

$$\tau_p \triangleq \tau_{ij}, \quad \begin{cases} \varepsilon_q \triangleq \varepsilon_{kl} & \text{for } q = 1,2,3, \\ \varepsilon_q \triangleq 2\varepsilon_{kl} & \text{for } q = 4,5,6. \end{cases}$$

As noted earlier the plate has orthotropic symmetry with respect to the co-ordinate axes, in which three-dimensional shear and extension are not coupled. In accordance with the work of Mindlin [7], the free development of the thickness plate strains $\varepsilon_{33}^{(0)} = u_3^{(1)}$ and $\varepsilon_{33}^{(1)} = 2u_3^{(2)}$ is allowed. This is accomplished by setting $\tau_{33}^{(0)} = \tau_{33}^{(1)} = 0$ in the plate constitutive equations, which are obtained by substituting from Eqs. (2) and (5) into Eq. (9), performing the integrations and employing Eq. (12). This permits the elimination of $\varepsilon_3^{(0)}$ and $\varepsilon_3^{(1)}$ in the two-dimensional

Table 1
Compressed matrix notation scheme

ij or *kl*	11	22	33	23 (or 32)	31 (or 13)	12 (or 21)
p or *q*	1	2	3	4	5	6

constitutive equations, which then may be written in the form

$$[\tau_1^{(k)}, \tau_2^{(k)}, \tau_4^{(k)}, \tau_5^{(k)}, \tau_6^{(k)}] = \hat{\Theta}^{(k,k)}[(c_{11}^* \varepsilon_1^{(k)} + c_{12}^* \varepsilon_2^{(k)}), (c_{12}^* \varepsilon_1^{(k)} + c_{22}^* \varepsilon_2^{(k)}), c_{44}\varepsilon_4^{(k)}, c_{55}\varepsilon_5^{(k)}, c_{66}\varepsilon_6^{(k)}], \quad k = 0, 1, \tag{14}$$

where

$$c_{11}^* = c_{11} - c_{13}^2/c_{33}, \quad c_{12}^* = c_{12} - c_{13}c_{32}/c_{33}, \quad c_{22}^* = c_{22} - c_{23}^2/c_{33} \tag{15}$$

are the two-dimensional elastic constants for the plate. Note that Eq. (14) shows that the plate constitutive equations are uncoupled for $k = 0$ and 1. Furthermore, all the higher order accelerations, i.e., $\ddot{u}_j^{(1)}$, $\ddot{u}_3^{(2)}$ may be ignored, since the frequencies are well below the lowest thickness resonant frequencies of the plate. In addition, $\tau_{a3}^{(n)}$, $\bar{F}_3^{(n)}$ for $n \geqslant 1$ are neglected in this lowest order approximation. With the foregoing approximations, from Eq. (8) the variational equation may be written in the form

$$\begin{aligned}
&\left[\int_S \mathrm{d}S\left(\tau_{ab,a}^{(0)} - 2\rho h\ddot{u}_b^{(0)}\right)\delta u_b^{(0)} - \int_{c_N} n_a\tau_{ab}^{(0)}\delta u_b^{(0)}\,\mathrm{d}s + \int_{c_C} u_b^{(0)}\delta\left(n_a\tau_{ab}^{(0)}\right)\mathrm{d}s\right] \\
&+ \left[\int_S \mathrm{d}S\left\{\left(\tau_{a3,a}^{(0)} - 2\rho h\ddot{u}_3^{(0)}\right)\delta u_3^{(0)} + \left(\tau_{ab,a}^{(1)} - \tau_{3b}^{(0)}\right)\delta u_b^{(1)}\right\}\right. \\
&\quad + \int_{c_C} \mathrm{d}s\left\{u_3^{(0)}\delta\left(n_a\tau_{a3}^{(0)}\right) - u_{3,b}^{(0)}\delta\left(n_a\tau_{ab}^{(1)}\right)\right\} \\
&\quad - \int_{c_N} \mathrm{d}s\left\{\left(n_a\tau_{a3}^{(0)} + \left(n_a\tau_{ab}^{(1)}s_b\right)_{,s}\right)\delta u_3^{(0)} - n_a\tau_{ab}^{(1)}n_b\delta u_{3,n}^{(0)}\right\} \\
&\quad \left. + \int_{c_N} \mathrm{d}s\left(n_a\tau_{ab}^{(1)}s_b\delta u_3^{(0)}\right)_{,s}\right] = 0,
\end{aligned} \tag{16}$$

where the subscripts n, s after commas represent the spatial derivatives along the normal and tangential directions of the edges, respectively, s_b denotes the component of the unit tangent vector to the curve of the edge in the counterclockwise direction, and the assumption of classical flexure has been employed, which is given in Eq. (19) below. Note that all the inhomogeneous terms in Eq. (16) have been ignored because they are not required in this treatment. Also note that in Eq. (16) the terms in the first bracket are for extension and those in the second are for flexure, which are uncoupled from each other as a consequence of Eqs. (16) and (14). Since in this work only the flexural portion of the variational equation in Eq. (16) is of interest, the extensional portion is taken to vanish. Consequently, only the flexural portion is to be understood hereafter whenever reference to Eq. (16) is made. A companion paper [12] treats the free in-plane vibrations

of a cantilevered rectangular plate. The last term in Eq. (16) results in Kirchhoff's corner conditions when the integration is performed and abrupt discontinuities in the normal occur at points [7]. It should be noted that they arise from an integration by parts around a c_N. Since Lagrange multipliers were used with constraint-type conditions in the principle from which Eq. (16) was derived [9], each variation in Eq. (16) is treated as unconstrained [10]. Hence, all the coefficients of the variations in Eq. (16) vanish independently, from which the plate differential equations, edge and corner conditions can be obtained. If the solution satisfying these conditions is obtained, the variational equation is satisfied exactly. However, since not all of the resulting equations can be satisfied exactly for the problem under consideration, the surface integral term in Eq. (16) is made to vanish first without considering any edge conditions. From the independence of $\delta u_3^{(0)}$ and $\delta u_b^{(1)}$, the equations

$$\tau_{a3,a}^{(0)} = 2\rho h\ddot{u}_3^{(0)}, \quad \tau_{ab,a}^{(1)} - \tau_{3b}^{(0)} = 0 \tag{17a, b}$$

are obtained. Since for the classical flexure of thin plates the wavelength along the plate is much larger than the thickness, Eq. (17b) shows that $|\tau_{3b}^{(0)}| \ll |\tau_{ab,a}^{(1)}|$. On account of this, the constitutive equations for $\tau_4^{(0)}$ and $\tau_5^{(0)}$ are ignored and Eq. (17b) is used instead. The substitution of Eq. (17b) into Eq. (17a) yields the classical form of the differential equation for the flexural vibrations of a thin plate in the form

$$\tau_{ab,ab}^{(1)} = 2\rho h\ddot{u}_3^{(0)}. \tag{18}$$

To complete the reduction and make Eq. (18) useful, the $u_b^{(1)}$ must be eliminated from the description. To this end, from the condition employed by Mindlin [7], which is that the plate shearing strain $\varepsilon_{3a}^{(0)} = 0$, the equation

$$u_a^{(1)} = -u_{3,a}^{(0)} \tag{19}$$

is obtained, which enables the elimination of $u_b^{(1)}$. Thus, at this point, one differential equation remains, i.e., Eq. (18), in one variable $u_3^{(0)}$, i.e., the deflection. Now from the independence of $\delta u_3^{(0)}$ and $\delta u_{3,n}^{(0)}$ along c_N, from Eq. (16) for free edges, two traction-free edge conditions

$$n_a\tau_{a3}^{(0)} + \left(n_a\tau_{ab}^{(1)}s_b\right)_{,s} = 0, \quad n_a\tau_{ab}^{(1)}n_b = 0 \tag{20}$$

are obtained.

From Eqs. (7), (17b) and (19), the stress resultant–plate displacement gradient relations are obtained in the form

$$\tau_{11}^{(1)} = -\hat{D}\left(u_{3,11}^{(0)} + \hat{\nu}u_{3,22}^{(0)}\right), \quad \tau_{22}^{(1)} = -\hat{D}\left(Ru_{3,11}^{(0)} + \hat{\nu}u_{3,22}^{(0)}\right), \tag{21}$$

$$\begin{aligned} \tau_{31}^{(0)} &= -\hat{D}\left(u_{3,11}^{(0)} + Tu_{3,22}^{(0)}\right)_{,1}, \quad \tau_{32}^{(0)} = -\hat{D}\left(Ru_{3,22}^{(0)} + Tu_{3,11}^{(0)}\right)_{,2}, \\ \tau_{12}^{(1)} &= -\hat{D}(T - \hat{\nu})u_{3,12}^{(0)}, \end{aligned} \tag{22}$$

which also result in

$$\tau_{31}^{(0)} + \tau_{12,2}^{(1)} = -\hat{D}\left(u_{3,111}^{(0)} + \hat{\mu}u_{3,122}^{(0)}\right), \quad \tau_{32}^{(0)} + \tau_{12,1}^{(1)} = -\hat{D}\left(Ru_{3,222}^{(0)} + \hat{\mu}u_{3,211}^{(0)}\right), \tag{23}$$

where

$$\hat{D} = 2h^3 c_{11}^*/3, \quad \hat{v} = c_{12}^*/c_{11}^*, \tag{24,25}$$

$$R = c_{22}^*/c_{11}^*, \quad T = \left(2c_{66}/c_{11}^*\right) + \hat{v}, \quad \hat{\mu} = (2T - \hat{v}). \tag{26–28}$$

3. Solution of the differential equation and edge conditions on the two traction-free opposite faces

As noted in the Introduction the problem of the free flexural vibrations of a cantilever plate with a fixed edge at $x_1 = -l$, and three free edges at $x_1 = l$, $x_2 = \pm b$, as shown in Fig. 1(a), cannot be solved exactly. At this point, it should be noted that although we have provided in Fig. 1(b) a differential element of the plate containing all the relevant stress resultants, we do not derive the flexural and extensional differential equations from the element, but instead derive the differential equations and edge conditions systematically from the variational formulation. This is done because although we solve much of the problem exactly, we ultimately leave a portion to be satisfied variationally and, consequently, we feel that the discourse will be clearer if all the equations and conditions that are satisfied exactly are obtained from the basic variational equation. Accordingly, in this work, this problem is treated by first obtaining the exact solution for low frequency flexural waves in a plate free at $x_2 = \pm b$. This results in a set of dispersion curves giving frequency versus wave number in the x_1 direction relations, which are determined in this section. In the next section a relatively small number of these waves is taken at a given frequency and substituted in what remains of the variational equation in Eq. (16), which is then satisfied to obtain the eigenmodes of vibration.

The substitution of Eqs. (21) and $(22)_3$ into Eq. (18) and the replacement of $u_3^{(0)}$ by w for notational convenience, yields the differential equation of the plate in the form

$$w_{,1111} + 2Tw_{,1122} + Rw_{,2222} + \hat{\kappa}^2 \ddot{w} = 0, \tag{29}$$

where

$$\hat{\kappa}^2 = 2\rho h/\hat{D}. \tag{30}$$

From Eq. (20) for the case at hand, the free edge conditions take the form

$$\tau_{23}^{(0)} + \tau_{21,1}^{(1)} = 0, \quad \tau_{22}^{(1)} = 0 \quad \text{at } x_2 = \pm b. \tag{31,32}$$

A solution of Eq. (29) may be written in the form

$$w = \Re\left\{A e^{\mathrm{i}(\omega t - \xi x_1 - \eta x_2)}\right\}, \tag{33}$$

where $\mathrm{i} = \sqrt{-1}$, A stands for an arbitrary constant and the symbol $\Re\{\}$ signifies the real part of the argument and will be dropped hereafter.

The solution in Eq. (33) satisfies Eq. (29) provided

$$\eta_{1,2}^2 = \frac{-T\xi^2 \pm \sqrt{(T^2 - R)\xi^4 + R\hat{\kappa}^2\omega^2}}{R}, \tag{34}$$

which shows that for a given ξ and ω, there are two independent η. Hence, the solution satisfying Eqs. (31) and (32), after the substitution of Eq. $(21)_2$ and Eq. $(23)_2$, can be written as

$$w(x_1, x_2, t) = \sum_{m=1}^{2}\sum_{n=1}^{2} C_{mn} \sin\{\eta_m x_2 + (n-1)\pi/2\} e^{i(\omega t - \xi x_1)}, \tag{35}$$

which includes waves either antisymmetric ($n = 1$) or symmetric ($n = 2$) in x_2, and C_{mn} denote arbitrary constants. The substitution of Eq. (35) into Eqs. (31) and (32) reveals that the symmetric and antisymmetric solutions uncouple and two sets of uncoupled simultaneous homogeneous linear algebraic equations are obtained, which may be written in the matrix form

$$\begin{bmatrix} (R\eta_1^2 + \hat{v}\xi^2)\sin\left\{\eta_1 b + \dfrac{(n-1)\pi}{2}\right\} & (R\eta_2^2 + \hat{v}\xi^2)\sin\left\{\eta_2 b + \dfrac{(n-1)\pi}{2}\right\} \\ \eta_1(R\eta_1^2 + \hat{\mu}\xi^2)\cos\left\{\eta_1 b + \dfrac{(n-1)\pi}{2}\right\} & \eta_2(R\eta_2^2 + \hat{\mu}\xi^2)\cos\left\{\eta_2 b + \dfrac{(n-1)\pi}{2}\right\} \end{bmatrix} \begin{bmatrix} C_{1n} \\ C_{2n} \end{bmatrix} = \begin{bmatrix} 0 \\ 0 \end{bmatrix}, \tag{36}$$

where $n = 1,\ 2$ for the antisymmetric and symmetric waves, respectively.

For the purpose of calculation, it is convenient to write the equations involved in the calculation in terms of dimensionless variables, which are defined by

$$\begin{aligned} &\bar{\xi} = 2b\xi/\pi, \quad \bar{\eta}_r = 2b\eta_r/\pi, \quad \bar{x}_a = \pi x_a/(2b), \\ &\bar{\Omega} = \omega/\bar{\omega}, \quad \tau = \bar{\omega}t, \quad r = 1, 2, \end{aligned} \tag{37}$$

where

$$\bar{\omega} = \frac{\pi}{2b}\sqrt{\frac{c_{66}}{\rho}}. \tag{38}$$

For a non-trivial solution of Eq. (36), the determinant of the matrix must vanish, which yields the two transcendental dispersion relations

$$\frac{\tan(\pi\bar{\eta}_m/2)}{\tan(\pi\bar{\eta}_n/2)} = \frac{\bar{\eta}_2(R\bar{\eta}_1^2 + \hat{v}\bar{\xi}^2)(R\bar{\eta}_2^2 + \hat{\mu}\bar{\xi}^2)}{\bar{\eta}_1(R\bar{\eta}_2^2 + \hat{v}\bar{\xi}^2)(R\bar{\eta}_1^2 + \hat{\mu}\bar{\xi}^2)}, \tag{39}$$

where $(m, n) = (1, 2)$ for the symmetric waves and $(m, n) = (2, 1)$ for the antisymmetric waves.

From either of the equations in Eq. (36), the amplitude ratios are obtained in the form

$$\bar{C}_{1n}(\bar{\xi}) = -(R\bar{\eta}_2^2 + \hat{v}\bar{\xi}^2)\sin\{\pi(\bar{\eta}_2 + n - 1)/2\}, \tag{40a}$$

$$\bar{C}_{2n}(\bar{\xi}) = (R\bar{\eta}_1^2 + \hat{v}\bar{\xi}^2)\sin\{\pi(\bar{\eta}_1 + n - 1)/2\}, \tag{40b}$$

where subscript $n = 1, 2$ for the antisymmetric and the symmetric modes, respectively.

The cut-off frequencies are obtained by considering the solutions of Eq. (39) when $\bar{\xi} = 0$ but $\bar{\Omega} \neq 0$, which yields

$$\frac{\tan\left(\pi\sqrt{\bar{\kappa}\,\bar{\Omega}}/2\right)}{\tanh\left(\pi\sqrt{\bar{\kappa}\,\bar{\Omega}}/2\right)} = \pm 1, \tag{41}$$

where

$$\bar{\kappa} = \left(\frac{b}{\pi h}\right)\sqrt{\frac{6(T-\hat{v})}{R}} \tag{42}$$

and the positive and negative signs on the right-hand side of Eq. (41) correspond to the antisymmetric and symmetric modes, respectively. Note that for an isotropic material, $R = T = 1$, and $\hat{v}, \hat{D}$ can be, respectively, replaced with the usual Poisson's ratio v and flexural rigidity D in all the related equations.

Even though there are an infinite number of solutions at $\bar{\Omega} = 0$, they cannot be obtained from Eq. (39) in the isotropic case[1] because then only one independent η is obtained from Eq. (34). However, in the isotropic case, the solutions can be obtained by using Eq. (39) and taking the limit as $\bar{\Omega}$ approaches zero from above, with the result

$$\lim_{\bar{\Omega}\to 0}\frac{\partial\Phi(\bar{\xi},\bar{\Omega})}{\partial\bar{\Omega}} - \lim_{\bar{\Omega}\to 0}\frac{\partial\Psi(\bar{\xi},\bar{\Omega})}{\partial\bar{\Omega}} = 0, \tag{43}$$

where

$$\Psi(\bar{\xi},\bar{\Omega}) = \frac{\bar{\eta}_2\left(\bar{\eta}_1^2 + v\bar{\xi}^2\right)\left\{\bar{\eta}_2^2 + (2-v)\bar{\xi}^2\right\}}{\bar{\eta}_1\left(\bar{\eta}_2^2 + v\bar{\xi}^2\right)\left\{\bar{\eta}_1^2 + (2-v)\bar{\xi}^2\right\}}, \tag{44}$$

$$\Phi(\bar{\xi},\bar{\Omega}) = \tan(\pi\bar{\eta}_m/2)/\tan(\pi\bar{\eta}_n/2), \tag{45}$$

which enable us to obtain the intersection of the complex branches with the plane $\bar{\Omega} = 0$.

Again, $(m, n) = (1, 2)$ for the symmetric waves and $(m, n) = (2, 1)$ for the antisymmetric waves. Eq. (41) for the cut-off frequencies and Eqs. (43)–(45) for the limiting case when $\bar{\Omega}$ approaches zero can significantly aid the calculation by determining starting points to get on dispersion curves, after which Eq. (39) are used to obtain the remainder of the dispersion curves.

4. Variational approximation

Since the solution function Eq. (35) satisfies the differential Eq. (18) and free boundary conditions at $\bar{x}_2 = \pm\pi/2$ exactly, all that remains in Eq. (16) is

$$\begin{aligned} -\int_{-b}^{b} \mathrm{d}x_2 \Bigg[& \left[\left(\tau_{13}^{(0)} + \tau_{12,2}^{(1)}\right)\delta w - \tau_{11}^{(1)}\delta w_{,1}\right]_{x_1=l} \\ & + \left[w\delta\tau_{13}^{(0)} - w_{,1}\delta\tau_{11}^{(1)} - w_{,2}\delta\tau_{12}^{(1)}\right]_{x_1=-l}\Bigg] \\ & - \left[\tau_{12}^{(1)}\delta w\right]_{x_1=-l,x_2=-b}^{x_1=-l,x_2=b} + 2\left[\tau_{12}^{(1)}\delta w\right]_{x_1=l,x_2=-b}^{x_1=l,x_2=b} = 0, \end{aligned} \tag{46}$$

[1] The analysis is performed for an orthotropic material because the solution for that symmetry is required in future work.

where

$$\tau_{11}^{(1)} = -\hat{D}(w_{,11} + \hat{\nu}w_{,22}), \quad \tau_{13}^{(0)} + \tau_{12,2}^{(1)} = -\hat{D}(w_{,111} + \hat{\mu}w_{,122}),$$
$$\tau_{12}^{(1)} = -\hat{D}(T - \hat{\nu})w_{,12}, \tag{47-49}$$

and the definition $[f(x)]_{x=p} = f(p)$ has been employed.

Note that the last two terms in Eq. (46) were obtained by performing the last line integral around c_N in Eq. (16) along the three free edges in the counterclockwise direction. The first of these arises from the integration along the two opposite free edges evaluated at the wall and the second and last of these in Eq. (46) came from the two jump conditions across the edges of discontinuity at $x_1 = l\ , x_2 = \pm b$, which are given by

$$-\llbracket n_a \tau_{ab}^{(1)} s_b\, \delta w \rrbracket_{x_1=l,x_2=-b} - \llbracket n_a \tau_{ab}^{(1)} s_b\, \delta w \rrbracket_{x_1=l,x_2=b}, \tag{50}$$

and where the jump notation

$$\llbracket g(x) \rrbracket_{x=q} \quad \text{for } g^+(q) - g^-(q),$$

has been introduced.

Even though all the branches obtained from the dispersion relation can be part of the solution for the plate bounded in the x_1 direction, inclusion of all branches is not only unreasonable, but also impossible since the dispersion relation includes an infinite number of imaginary and complex branches. However, since wave numbers having very large imaginary parts have a negligible influence on the frequency spectrum, they may be ignored in Eq. (35). Hence, the solution function having P dispersion branches can be written in the form

$$w(\bar{x}_1, \bar{x}_2, \tau) = \sum_{p=1}^{P} \sum_{q=1}^{2} \sum_{r=1}^{2} A_{pr} \bar{H}_{pqn} \sin\{\bar{\eta}_{pq}\bar{x}_2 + (n-1)\pi/2\}$$
$$\times \sin\{\bar{\xi}_p \bar{x}_1 + (r-1)\pi/2\}\, e^{i\bar{\Omega}\tau}, \tag{51}$$

where

$$\bar{H}_{pqn} = \bar{C}_{qn}(\bar{\xi}_p), \quad \bar{\eta}_{pq} = \bar{\eta}_q(\bar{\xi}_p) \tag{52}$$

are amplitude ratios and $n = 1, 2$ for the antisymmetric and the symmetric modes, respectively, and A_{pr} are arbitrary constants to be determined. Here, the amplitude A_{pr} can be a real, an imaginary or even a complex number since w is understood to be a real function. Special attention needs to be taken with the complex wave branches since both complex conjugate pairs must be included.

The substitution of Eqs. $(21)_1$, $(22)_1$, $(22)_3$ and $(23)_1$ into Eq. (46) yields

$$\int_{-\pi/2}^{\pi/2} d\bar{x}_2 \Big[\big[\big(w_{,111} + \hat{\mu}w_{,122}\big)\delta w - \big(w_{,11} + \hat{\nu}w_{,22}\big)\delta w_{,1} \big]_{\bar{x}_1=\pi l/(2b)}$$
$$+ \big[w\delta\big(w_{,112} + Tw_{,222}\big) - w_{,1}\delta\big(w_{,11} + \hat{\nu}w_{,22}\big) - (T - \hat{\nu})w_{,2}\delta w_{,12} \big]_{\bar{x}_1=-\pi l/(2b)} \Big]$$
$$+ (T - \hat{\nu}) \Big\{ \big[w_{,12}\delta w \big]_{\bar{x}_1=-\pi l/(2b),\bar{x}_2=-\pi/2}^{\bar{x}_1=-\pi l/(2b),\bar{x}_2=\pi/2} - 2\big[w_{,12}\delta w \big]_{\bar{x}_1=-\pi l/(2b),\bar{x}_2=-\pi/2}^{\bar{x}_1=\pi l/(2b),\bar{x}_2=\pi/2} \Big\} = 0, \tag{53}$$

which is all that remains in the variational equation and where the indices following the commas represent the derivatives with respect to the dimensionless spatial co-ordinates $\bar{x}_a$.

The substitution of Eq. (51) into Eq. (53) along with the integration and evaluation called for yields two independent sets of homogeneous algebraic equations, corresponding to the symmetric and antisymmetric modes. Each set of equations consists of $2P$ equations with $2P$ unknowns, which may be written in the matrix form

$$\mathbf{KX} = \mathbf{0}, \tag{54}$$

where $\mathbf{K}$ is a $2P \times 2P$ matrix and $\mathbf{X}$ is a $2P$ unknown magnitude vector with

$$A_{pr} = X_{2(p-1)+r}. \tag{55}$$

The vanishing determinant of $\mathbf{K}$ yields the characteristic equations of the antisymmetric and symmetric modes of the plate motion along with amplitude ratios from any $2P-1$ of the consistent homogeneous equations. The amplitude ratios Eq. (55) along with the solution function Eq. (51) yield the mode shapes of the plate for any antisymmetric or symmetric mode.

5. Discussion of results

Even though the equations derived hold for the plate of orthotropic material (see footnote 1), the numerical computation was performed for the isotropic material to enable comparison with the results of Ref. [1]. Since the dispersion curves in the proper wave number range are required before the eigenmodes obtained in Section 4 can be calculated, the calculation of the dispersion curves naturally was performed first, and is shown in Fig. 2. Computations were made separately using quadruple precision and a symbolic math package Maple [13] to reduce possible errors caused by the large imaginary parts of the wave numbers. Here, $\Re(\bar{\xi})$ and $\Im(\bar{\xi})$ represent real and imaginary, respectively. As expected, the complex wave numbers appear in conjugate pairs, which are known to be associated with edge vibrations in a bounded plate [14]. By using the calculated dispersion relations, which are basically a function of the Poisson's ratio only for the isotropic material, natural frequencies and mode shapes were calculated for various length-to-width ratios. In order to compare results, the same combinations of aspect ratios and the Poisson's ratio, which is 0.3, were chosen as in Ref. [1].

Comparison was also made with the results obtained with P3/PATRAN [8], a commercial finite element package. For the FEM, around 800–1200 quadrilateral elements with four nodes were adopted using the subiteration method [8]. Before making the detailed calculations, a number of convergence tests were performed, as can be seen in Table 2. In the table, the natural frequencies obtained by including 3, 5, and 7 branches were compared to those obtained by including nine branches for the first two symmetric modes. Clearly, the convergence is very fast for the first two symmetric modes. This shows that the real branches in Fig. 2(a) essentially determine those modes. Moreover, the real branches in Figs. 2(a) and (b) are by far the largest part of all the modes calculated.

Although the results of calculations shown in Table 3 are for l/b ratios of $\frac{5}{2}$, $\frac{3}{2}$, 1, $\frac{2}{3}$ and $\frac{2}{5}$, the analysis presented in this work should not really be used for l/b ratios significantly less than 1 because then the edge conditions satisfied exactly are over a smaller region than those satisfied

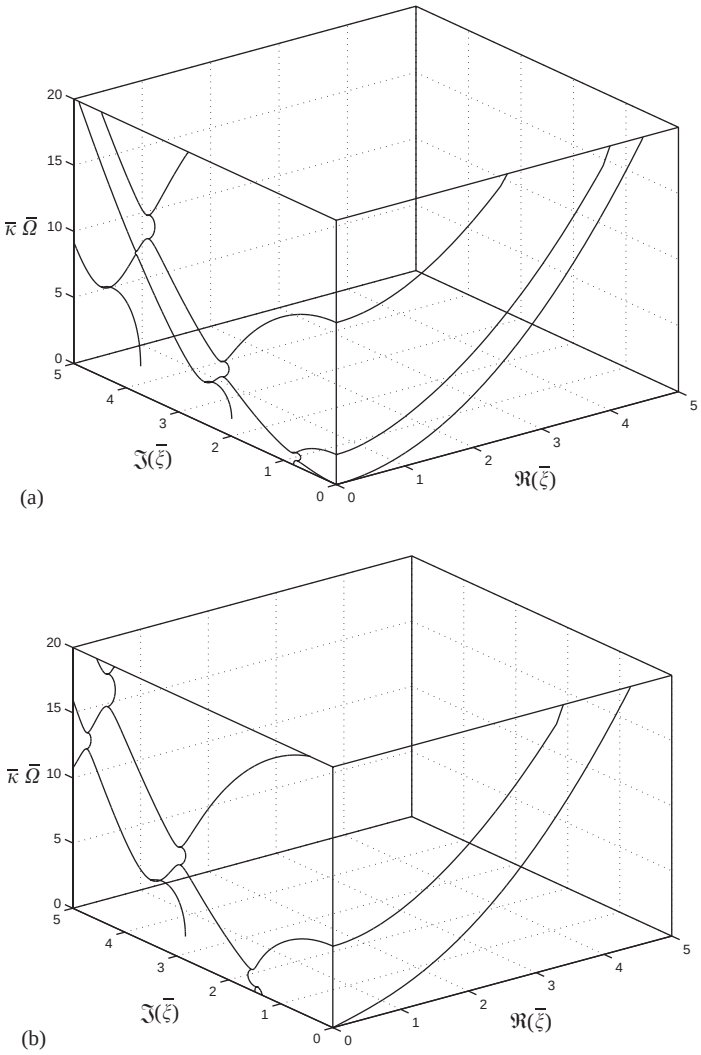

Fig. 2. Dispersion curves for the out-of-plane motion of the rectangular cantilever plate: (a) for symmetric modes and (b) for antisymmetric modes.

variationally. When $l/b<1$ the edge conditions at the fixed edge and the free-cantilevered edge should be satisfied exactly and the conditions on the free opposite edges should be satisfied variationally. However, when this is done the waves that determine the dispersion curves become asymmetric and a much larger number of dispersion curves must be included to make any calculation. Rather than doing this additional work, the solution was used for ratios $l/b<1$ and the accuracy of the results was extremely surprising, as evidenced by the comparison with the finite element method P3/PATRAN calculation and Leissa's Rayleigh–Ritz calculation [1], as shown in Table 3. That is the reason the results for $l/b<1$ are presented in the table.

Eigenvalues computed for the first six modes of the cantilever plate using the treatment presented in this work are shown in Table 3 along with the results of Ref. [1] and the

Table 2
Convergence tests for the out-of-plane motion of the rectangular cantilever plate for the first two symmetric modes ($l/b = \frac{5}{2}$): S_1 = first symmetric mode; S_2 = second symmetric mode; N( ) = natural frequency $\bar{\kappa}\bar{\Omega}$ (ND) of ( ), R(%) = N (specified number of branches included)/N(9 branches included) × 100

Included branch #		Mode	
		S_1	S_2
3	N	0.05461	0.34580
	R	98.36	99.76
5	N	0.05534	0.34625
	R	99.68	99.89
7	N	0.05548	0.34651
	R	99.93	99.96
9	N	0.05552	0.34664
	R	100.00	100.00

Table 3
Dimensionless natural frequencies for the out-of-plane motion of the rectangular cantilever plate and their comparison with Leissa [1] and P3/PATRAN [8]

Mode #	l/b														
	2/5			2/3			1			3/2			5/2		
1	C_7	2.2055	S	C_7	0.7915	S	C_7	0.3506	S	C_7	0.1551	S	C_7	0.0555	S
	L	2.2232		L	0.7985		L	0.3538		L	0.1566		L	0.0560	
	P	2.2115		P	0.7961		P	0.3518		P	0.1555		P	0.0557	
2	C_5	3.0103	A	C_5	1.4540	A	C_5	0.8610	A	C_5	0.5245	A	C_5	0.2911	A
	L	3.0309		L	1.4604		L	0.8637		L	0.5258		L	0.2916	
	P	3.0190		P	1.4581		P	0.8607		P	0.5248		P	0.2910	
3	C_7	5.0877	S	C_7	3.2917	S	C_7	2.1547	S	C_7	0.9657	S	C_7	0.3465	S
	L	5.1386		L	3.3143		L	2.1712		L	0.9735		L	0.3496	
	P	5.1063		P	3.2963		P	2.1668		P	0.9630		P	0.3467	
4	C_7	8.7122	A	C_7	4.9916	S	C_7	2.7537	S	C_5	1.7695	A	C_5	0.9272	A
	L	8.7909		L	5.0241		L	2.7692		L	1.7784		L	0.9315	
	P	8.7341		P	5.0094		P	2.7631		P	1.7670		P	0.9287	
5	C_7	13.766	S	C_5	5.8773	A	C_5	3.1316	A	C_7	2.4103	S	C_7	0.9740	S
	L	13.702		L	5.9440		L	3.1522		L	2.4261		L	0.9821	
	P	13.666		P	5.9039		P	3.1607		P	2.4473		P	0.9764	
6	C_8	14.699	S	C_5	7.1534	A	C_7	5.4805	S	C_7	2.7731	S	C_5	1.7164	A
	L	15.028		L	7.2080		L	5.5162		L	2.7917		L	1.7172	
	P	14.536		P	7.1562		P	5.4865		P	2.7741		P	1.7175	

S: symmetric mode; A: antisymmetric mode; N( ) = natural frequency $\bar{\kappa}\bar{\Omega}$ (ND) of ( ); C_n (ND) = N (current research) with n dispersion branches included; L (ND) = N (Leissa); P (ND) = N (P3/PATRAN).

Table 4
Dimensionless natural frequencies of cantilever E–B beam and their comparison with the corresponding solutions of current research ($l/b = \frac{5}{2}$): N( ) = natural frequency $\bar{\kappa}\bar{\Omega}$ (ND) of ( ); EB (ND) = N (E–B beam)

$\bar{\kappa}\bar{\Omega}$	Mode#				
	1	2	3	4	5
C_7	0.0555	0.3465	0.9740	1.9096	3.0569
EB	0.0544	0.3408	0.9541	1.8697	3.0908

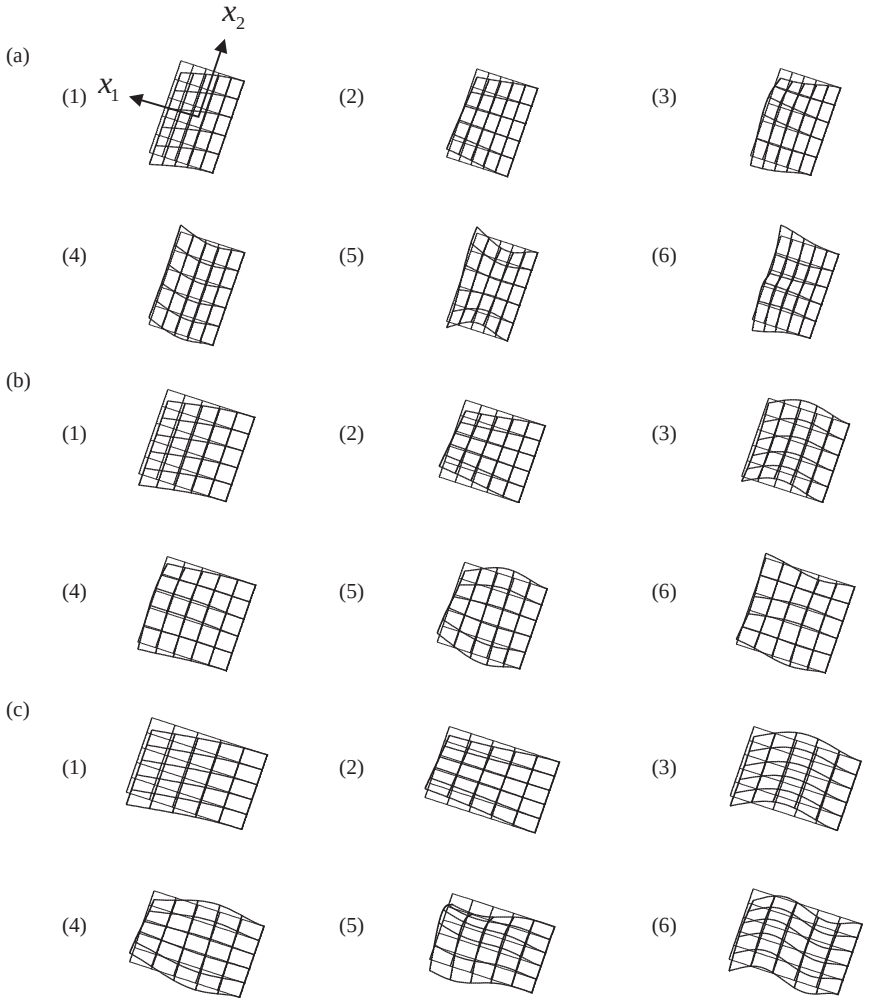

Fig. 3. First six mode shapes for the out-of-plane motion of the rectangular cantilever plate with various length-to-width ratios: (a) $l/b = \frac{2}{3}$, (b) $l/b = 1$ and (c) $l/b = \frac{3}{2}$.

P3/PATRAN calculation. In the calculation based on our treatment a total of seven dispersion branches for the symmetric modes and five for the antisymmetric modes, including the two real branches in the frequency range of interest, were included in most of the cases. The number of

branches used was determined by the fact that the largest imaginary wave number that could be included put restrictions on the number because of numerical precision. The table shows that the results of this research are in good agreement especially with those of P3/PATRAN. In general, the results of Ref. [1] are the largest of the three. Comparison of the natural frequencies for the available symmetric modes of the current work for $l/b = \frac{5}{2}$ with the solutions obtained from the Euler–Bernoulli (E–B) beam is also made in Table 4. As can be observed the difference between the two solutions easily exceeds 2% even for the fundamental modes.

Typical mode shapes are depicted in Fig. 3. The meandering shape on the fixed boundary is a result of the fact that the boundary conditions are satisfied approximately by integrating what remains of the variational equation over the fixed boundary and the free boundary opposite it, whereas the conditions on other edges are satisfied exactly. If the plate has an internal surface of discontinuity, the variational principle adopted here can be easily extended simply by including Lagrange multipliers at the interface.

References

[1] A.W. Leissa, The free vibration of rectangular plates, Journal of Sound and Vibration 31 (3) (1973) 257–293.
[2] S.F. Bassily, S.M. Dickinson, On the use of beam functions for problems of plates involving free edges, Journal of Applied Mechanics 42 (1975) 858–864.
[3] R.B. Bhat, Natural frequencies of rectangular plates using characteristic orthogonal polynomials in Rayleigh–Ritz method, Journal of Sound and Vibration 102 (4) (1985) 493–499.
[4] R.E. Rossi, P.A.A. Laura, Symmetric and antisymmetric normal modes of a cantilever rectangular plate: effect of Poisson's ratio and a concentrated mass, Journal of Sound and Vibration 195 (1) (1996) 142–148.
[5] D.J. Gorman, Free vibration analysis of cantilever plates by the method of superposition, Journal of Sound and Vibration 49 (4) (1976) 453–467.
[6] D.J. Gorman, Accurate free vibration analysis of the orthotropic cantilever plate, Journal of Sound and Vibration 181 (4) (1995) 605–618.
[7] R.D. Mindlin, An introduction to the mathematical theory of the vibration of elastic plates, US Army Signal Corps Engineering Laboratory, Fort Monmouth, NJ, Sec. 6.04, 1955.
[8] P3/PATRAN™, User Manual Release 1.2, PDA Engineering-PATRAN Division, 1993.
[9] H.F. Tiersten, Linear Piezoelectric Plate Vibrations, Plenum Press, New York, 1969, Sec. 6.4 (6.44) without the electrical terms and the integral over $S^{(d)}$, since it is for only one region.
[10] F.B. Hildebrand, Methods of Applied Mathematics, 2nd Edition, Prentice-Hall, Englewood Cliffs, NJ, 1965, p. 219, Problem 100.
[11] H.F. Tiersten, Linear Piezoelectric Plate Vibrations, Plenum Press, New York, 1969, Sec. 7.1.
[12] Jongwon Seok, H.F. Tiersten, H.A. Scarton, Free vibrations of rectangular cantilever plates. Part 2: in-plane motion, Journal of Sound and Vibration 271 (1–2) (2004) 147–158, this issue.
[13] Maple™, User Manual Release 5, Waterloo Maple Inc., 1997.
[14] D.C. Gazis, R.D. Mindlin, Extensional vibrations and waves in a circular disk and semi-infinite plate, Journal of Applied Mechanics 27 (1960) 541–547.